Dilute Solution Properties of Poly[*N*-(*n*-octadecyl)maleimide]. 1. Determination of Molecular Weight Distribution by Coacervation and Gel Permeation Chromatography

José M. Barrales-Rienda and Carmen Romero Galicia

Instituto de Plásticos y Caucho, CSIC, Madrid 6, Spain

Arturo Horta*

Departamento de Química General y Macromoléculas, Facultad de Ciencias, Universidad a Distancia (UNED), Madrid 3, Spain. *Received April 15, 1982*

ABSTRACT: The molecular weight distribution (MWD) of the title polymer is analyzed by combining the techniques of fractional coacervation and gel permeation chromatography (GPC). Twenty-four fractions of the original polymer have been obtained, and their number-average molecular weights (in the range M_n = 1.25×10^3 to 1.9×10^5) have been measured by membrane and vapor pressure osmometry. The cumulative fractionation data are fitted by the two-parameter MWD functions of Tung and of Wesslau. Gel permeation chromatograms of the fractions and of the original polymer have been determined, and the polydispersities of the fractions and the MWD of the polymer are obtained from these chromatograms. The analysis of GPC data is carried out by means of a nonlinear calibration of log M_n vs. elution volume at the peak, V_e(peak). The calibration is determined by an iterative computer method devised for use with polydisperse samples. The universal GPC calibration of log V_h (hydrodynamic volume) vs. V_e(peak) is also tested for its validity in the case of the comblike structure of our polymer. The results of fractional coacervation and of GPC are in fair agreement with regard to the MWD of the polymer.

Introduction

Poly[*N*-(*n*-octadecyl)maleimide] (PMI-18) is a typical comblike polymer, with structural unit I. The backbone

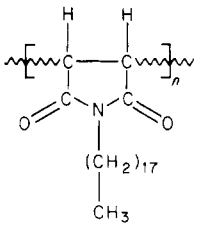

I

of this polymer is semistiff because of the steric hindrances created by the two successive 2,5-dioxopyrrolidone-3,4-diyl rings. Polymers of this type offer very interesting possibilities when their properties in dilute solution and in the solid state are studied as a function of molecular weight. For such studies, well-characterized samples having narrow molecular weight distributions (MWD) are required. No detailed studies on the fractionation and MWD of these polymers have yet been carried out. It is to this task that we address ourselves in the present paper, the first in a series on the dilute solution properties of PMI-18. We discuss here the application of fractional coacervation and gel permeation chromatography (GPC) to fractionate the polymer and to characterize the polydispersity of the fractions. The results from both methods (coacervation and GPC) are used in parallel to obtain the MWD of PMI-18.

The interpretation of results from GPC on PMI-18 may be more complicated than in the case of other linear vinyl or acrylic polymers because PMI-18 has not only a rather stiff backbone but also long *n*-alkyl side chains. While the presence of chain stiffness seems to have no special effect on GPC, side chains of comblike polymers may affect GPC appreciably. An additional difficulty may arise from the solute–gel interaction known for nitrogen-containing polymers,[1,2] which could affect elution volumes and disturb the reliability of M_w/M_n values calculated from the chromatograms (M_n and M_w being number- and weight-average molecular weights, as usual).

The simultaneous application of coacervation and GPC to obtain the MWD allows for comparison between the methods and provides more information than either method separately.

The MWD can be obtained from GPC provided a relation between molecular weight and elution volume can be adequately established[3-10] by using standard samples or the universal calibration approach based on the hydrodynamic volume concept of Benoit et al.[11,12] The calibration is readily obtained if well-characterized samples of the polymer under investigation are available. If possible, the fractions should have a low polydispersity index, i.e., M_w/M_n = 1.1. For some polymers this is not always attainable because of the long duration and inefficiency of most polymer fractionation techniques. With polydisperse samples no direct relationship between average molecular weights and peak elution volumes holds, and more elaborate numerical methods are needed to obtain the calibration. We follow here one such numerical method that makes use of the experimentally determined chromatograms and M_n values of the fractions.

Comparisons of molecular weight averages obtained by osmometry and light scattering, namely, M_n and M_w, with those obtained by GPC are scarce. In general, agreement is not as good as desirable. Thus indirect comparisons made from the point of view of molecular weight distribution carried out by GPC and fractional precipitation have shown some significant differences.[13-20] A more rigorous comparison will be required if we wish to make more precise and conclusive comparisons by the different procedures.

Thus far there have been no absolute comparisons in the literature between MWD's calculated by GPC and by other fractionation methods for the same whole polymer sample and its fractions in terms of distribution functions and number- and weight-average molecular weights for each of the fractions. Many of the possibilities of GPC have yet to be elucidated. Probably one of the most interesting tests of the usefulness of the technique can be the comparison of MWD obtained by GPC with those derived from some other method of fractionation.

0024-9297/83/2216-0932$01.50/0

Table I
Fractional Coacervation Data of Poly[N-(n-octadecyl)maleimide] (PMI-18), Number-Average Molecular Weight (M_n), Elution Volume at the Peak (V_e(peak)), and Molecular Weight Averages $(M_w)_{GPC}$, $(M_n)_{GPC}$, and M_{GPC} Obtained from GPC Chromatograms of the Fractions

fraction no.	W_i, g	$w_i \times 10^2$	$I(M)$	$M_n \times 10^{-3}$	V_e(peak), mL	$(M_w)_{GPC} \times 10^{-3}$	$(M_n)_{GPC} \times 10^{-3}$	$\bar{M}_{GPC} \times 10^{-3}$
F-1	1.1168	3.3943	98.3017	190.0	106.5	206.5	118.7	241.1
F-2	1.2317	3.7435	94.7328	140.0	109.0	175.6	124.9	203.9
F-3	0.8161	2.4804	91.6209	118.0	110.0	168.5	119.3	196.6
F-4	0.9186	2.7919	88.9847	91.8	113.0	138.0	107.7	157.1
F-5	1.3220	4.0180	85.5798	90.3	114.0	124.3	91.4	143.9
F-6	1.8721	5.6899	80.7258	73.6	117.0	103.3	79.0	117.2
F-7	1.5697	4.7708	75.4955	65.0	119.5	89.1	69.5	100.3
F-8	2.0717	6.2965	69.9618	52.1	122.5	75.6	58.9	86.3
F-9	1.5387	4.6766	64.4753	44.0	125.5	56.2	42.3	64.3
F-10	1.2151	3.6930	60.2905	40.0	126.5	62.9	45.1	73.6
F-11	1.5770	4.7930	56.0475	33.7	129.5	46.5	35.2	53.6
F-12	2.1238	6.4549	50.4235	29.7	132.0	39.4	30.6	45.0
F-13	1.2999	3.9508	45.2207	27.1	134.5	33.0	25.7	37.5
F-14	1.1611	3.5289	41.4808	23.0	136.5	27.5	21.7	31.0
F-15	1.3707	4.1660	37.6334	17.8	139.0	23.0	18.2	25.8
F-16	1.1287	3.4308	33.8350	13.5	141.5	18.2	14.6	20.1
F-17	1.2807	3.8924	30.1734	12.2	144.0	14.8	12.0	16.2
F-18	1.4076	4.2781	26.0881	10.0	146.5	12.1	9.70	13.1
F-19	1.1797	3.5855	22.1563	9.0	149.0	9.79	7.98	10.4
F-20	0.9338	2.8381	18.9445	7.9	151.5	8.00	6.06	8.46
F-21	1.7018	5.1723	14.9393	5.4	155.0	5.78	4.79	6.00
F-22	1.3941	4.2371	10.2346	3.7	157.0	4.46	3.73	4.62
F-23	1.9801	6.0181	5.1070	2.3	161.5	2.83	2.27	2.95
F-24	0.6903	2.0980	1.0490	1.25	165.5	1.73	1.36	1.81

In addition, there are several possible operating effects that can introduce errors in the GPC measurements. Steric exclusion is generally the predominant separation mechanism in GPC. However, adsorption on the gel, dissolution inside the gel, and incompatibility also may occur, greatly disturbing solute exclusion and especially making inadequate universal calibration for polymers with polar groups in their chemical structures.[21-23]

Keeping all this in mind, we may adopt a GPC procedure and treatment of data in which the column or a set of columns is calibrated to furnish a relationship of the elution volume to molecular weight of the samples. Samples of unknown molecular weight are then run and the molecular weight data are calculated by using the self-established calibration curve. Typically, the calibration curve under these circumstances is self-generated by using standards of the same polymer having molecular weight polydispersities as narrow as possible.

Experimental Section

Monomer Synthesis. *N*-(*n*-Octadecyl)maleimide monomer was prepared by reaction of maleic anhydride (Ferosa, S. A., Barcelona) with freshly recrystallized *n*-octadecylamine (Fluka, A. G.) according to a standard reaction method previously described.[24] The resulting monomer was purified by repeated crystallization. Physical constants are in agreement with those described for this monomer elsewhere.[24] Data from elemental analysis and ^{1}H NMR and IR spectra were in agreement with those expected from the structure.

Polymer Synthesis. All operations involved in the preparation of the polymerization reaction in bulk were made under high vacuum (10^{-5} mmHg). Polymerization was carried out in a sealed glass ampule under vacuum with 2,2′-azobis(isobutyronitrile) (AIBN) as initiator (2.0% w/w) in a silicone oil bath controlled at 100 ± 0.2 °C for 48 h.

The PMI-18 sample was recovered by washing the contents of the ampule with small amounts of toluene into 2000 mL of cold methyl alcohol. The sample was then isolated by filtration and dried to constant weight at 40 °C (10^{-5} mmHg). A white-yellowish fine powder was obtained. Conversion of *n*-octadecylmaleimide into polymer was 67.0%.

Purification was achieved by repeated dissolution and precipitation followed by drying under vacuum. The sample obtained after the last purification was also examined by elemental analysis and by both ^{1}H NMR and IR spectroscopy to verify the structure and purity of the sample. They were in agreement with the linear polymer structure and composition.

Fractional Coacervation. Toluene/methanol was employed as the solvent/coacervant system. The coacervation was carried out by a conventional procedure, starting with a 4.0% toluene solution (34.1 g/852.5 mL). Addition of coacervant up to cloudiness was followed by dissolution and thermal reequilibration at 20 °C. The fractions coacervated in a concentrated solution state. They were redissolved in toluene, precipitated with methanol, and subsequently dried at 40 °C (10^{-5} mmHg) for 24 h. The fractional coacervation data are given in Table I (columns 1–3), where W_i is weight in grams and w_i is weight fraction, that is, W_i divided by the sum of grams recovered in all the fractions. Yield of the fractionation, 96.5%.

Osmotic Pressure and Vapor Pressure Measurements. In the range of high molecular weight fractions a Hewlett-Packard Model 501 high-speed membrane osmometer was employed to determine the number-average molecular weight. Measurements were made at 25 °C for toluene solutions with a preconditioned Ultracella filter membrane. The number-average molecular weight was calculated by plotting $(\Pi/c)^{1/2}$ vs. c.

The number-average molecular weights of the ten lowest molecular weight fractions were measured by determining the vapor pressure lowering over their solutions in benzene at 30 °C. Measurements were made in duplicate on a Hitachi Perkin-Elmer Model 115 vapor pressure osmometer, using benzil as the calibration standard. Average values of quintuplicate determinations of ΔR were taken on each of the five selected concentrations and used to calculate the $\Delta R/c$ values. Number-average molecular weights were obtained by plotting $\Delta R/c$ vs. c (c expressed in grams per 1000 g of solvent) and dividing K (the calibration constant obtained in the same way and under the same experimental conditions) by the ordinate intercepts: $K/(\Delta R/c)_{c\to 0} = M_n$.

Values of M_n estimated by both osmotic pressure and vapor pressure osmometry are summarized in the fifth column of Table I. In the range where number-average molecular weights may be estimated by both vapor pressure and membrane osmometry, in other words, in the zone where the limits of detection of both techniques overlap, the agreement of M_n measured by the techniques was quite good, deviations being less than 5%.

Gel Permeation Chromatography Measurements. GPC experiments were performed at 25 °C on a Waters Associates Model 200 gel permeation chromatograph, with tetrahydrofuran

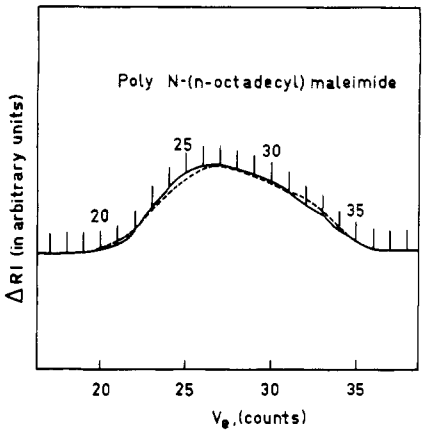

Figure 1. Gel permeation chromatogram trace of the whole PMI-18 polymer under experimental conditions indicated in the text at 25 °C and with THF as eluent. The dashed line represents base line adjustment chromatograms of PMI-18 fractions F-1 to F-24 made as indicated in the text. Data were calculated from individual GPC traces from each of the fractions obtained by fractional coacervation.

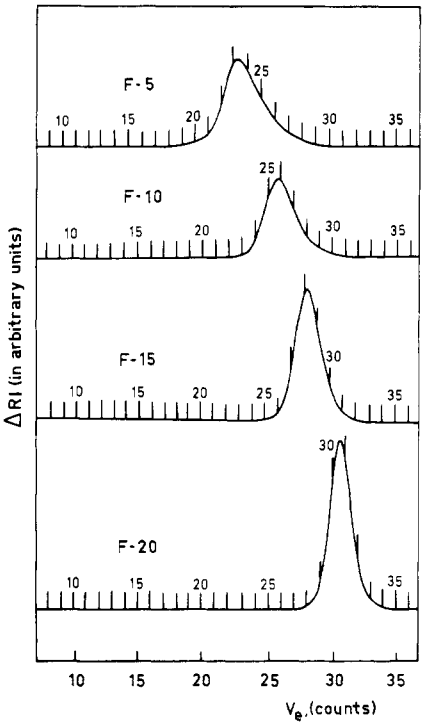

Figure 2. Gel permeation chromatography traces of the fractions F-5, F-10, F-15, and F-20 under the same experimental conditions used to obtain the GPC trace for the whole PMI-18 sample given in Figure 1.

(THF) as eluent. THF employed as the solvent was distilled from copper(I) chloride and potassium hydroxide. A series arrangement of five polystyrene columns, with upper porosity ratings of 10^3, 3×10^3, 3×10^4, 3×10^4, and 10^5 Å (Waters designation), was used. Elutions were conducted with a flow rate of 1 mL/min. Elution volume (counts) was calculated from the initial point of injection to the appearance of the peak height maximum of the GPC trace. Polymer concentrations (w/v) were as follows: PMI-18 fractions, 0.2–0.3%; polystyrene standards (PS), 0.2%. (All of the polymer in the sample loop (2 mL) was injected). The PS standards used to obtain the PS calibrations were supplied by Waters Associates and Pressure Chemical Co. The peak molecular weights (M(peak) = $(M_w M_n)^{1/2}$) quoted by the two companies for their respective PS standards were used to establish the PS calibration.

Figures 1 and 2 respectively show the GPC chromatograms of the whole polymer (PMI-18) and of some of the fractions obtained by fractional coacervation (only the chromatograms for fractions

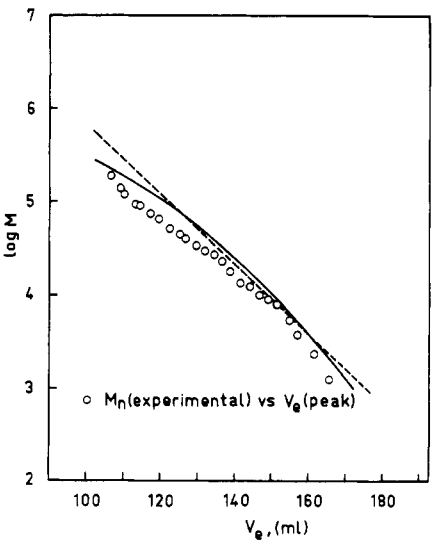

Figure 3. GPC calibration curves from the PMI-18 fractions: open circles, experimental results of log M_n(exptl) vs. elution volume at the peak, V_e(peak); full line, calibration curve fitted to the experimental results with a second-degree polynomial; dashed line, calibration curve fitted to the experimental results with a first-degree polynomial.

F-5, F-10, F-15, and F-20 are shown). It is evident that in these selected cases the fractions do not overlap extensively. It can also be observed as a general rule that the first few fractions, as may be the case for F-5, contain larger amounts of low and high molecular weight materials. In other words, the polydispersity index decreases with decreasing molecular weight of the fractions, as we will see later. The abscissa is time, with each count number representing an interval of 5 min or 5 mL of eluent. A plot of log M_n against elution volume at the peak, V_e(peak), is given by open circles in Figure 3.

The response of the differential refractometer detector is proportional to polymer concentration if the refractive index for a given polymer is independent of molecular weight. This is valid in the zone of high molecular weights but it does not hold at low molecular weights.[25] Therefore when the detector is intended to be applied at low molecular weights for absolute values of concentration, it is necessary to determine the detector response as a function of molecular weight. This correction has been taken into account when the integral molecular weight distribution of the whole polymer is calculated according to Schulz's procedure[26,27] using GPC data.

Intrinsic viscosities for the PMI-18 fractions in THF at 25 °C needed to establish the universal calibration through the hydrodynamic volume concept[11,12] have been taken from part 2 of this series.[28]

Results and Discussion

The most common way of representing fractionation data is by constructing the integral MWD according to a method originally developed by Schulz and Dinglinger.[26,27] According to these authors half the weight of a fraction is assumed to be composed of molecules possessing molecular weights lower than its molecular weight average and the other half is considered to be higher. Under this assumption the cumulative weight fraction $I(M)$ for the ith fraction is calculated from

$$I(M) = (1/2)w_i + \sum_{j=1}^{i-1} w_j \qquad (1)$$

For the whole polymer $I(M)$ was calculated according to eq 1 for all fractions using data from fractional coacervation. The integral distribution is shown as open circles in Figure 4. The integral distribution obtained directly from GPC gives almost the same values without any noticeable discrepancy. Keeping this in mind, we have omitted them on the graph.

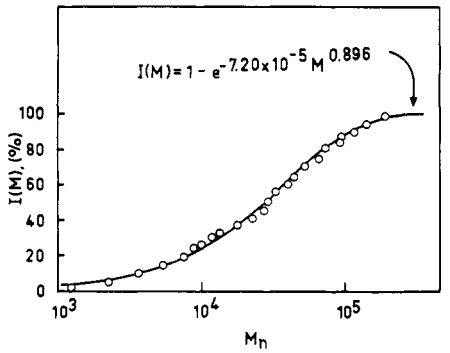

Figure 4. Cumulative weight distribution function calculated by Schulz's method vs. number-average molecular weight, M_n, plotted on a semilogarithmic scale using data for 24 fractions of PMI-18 obtained by fractional coacervation. Full line represents the integral distribution function and has been drawn by Tung's expression with $y = 7.20 \times 10^{-5}$ and $z = 0.896$ (obtained by the method of Tung in the linearized form plotted in Figure 5).

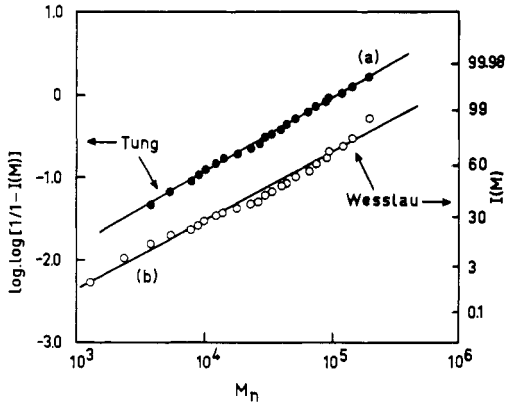

Figure 5. Fractional coacervation data of PMI-18 fractions plotted on (a) semilogarithmic graph paper according to the method of Tung in linearized form and (b) log-probability graph paper following a method developed by Wesslau.

Tung[29] has shown that a number of S-shaped integral distribution curves may be fitted by the following empirical equation:

$$I(M) = 1 - \exp(-yM^z) \quad (2)$$

where y and z are two adjustable constants; z varies inversely with the breadth of the distribution. Both y and z determine the location of the maximum. The Tung[29] distribution may be written in linearized form as

$$\log \log [1/1 - I(M)] = \log (y/\ln 10) + z \log M \quad (3)$$

Then a plot of log $[1/1 - I(M)]$ against M on a double-logarithmic scale will result in a straight line whose intercept and slope will yield y and z, respectively. Figure 5 shows such a plot of the PMI-18 fractionation data using $I(M)$ calculated by the Schulz summation method. The constants y and z obtained from the best straight line (correlation coefficient 0.998) are 7.20×10^{-5} and 0.896, respectively.

Differentiation of eq 2 gives the differential distribution function

$$d[I(M)]/dM = W(M) = yz \exp(-yM^z)M^{z-1} \quad (4)$$

This differential distribution $W(M)$ calculated from the fitted values of y and z is shown as a full line in Figure 6.

Once the parameters for the Tung[29] distribution function have been determined, the cumulative curve $I(M)$ may be drawn as a continuous function of M in Figure 4. The S shape of the experimental integral distribution obtained

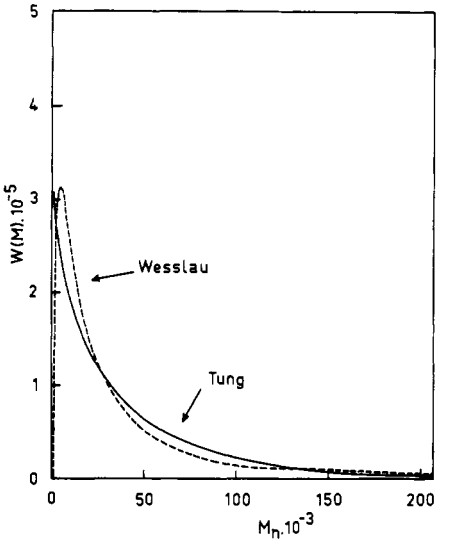

Figure 6. Differential weight distribution curves of PMI-18 obtained from fractionation data. Full line, by the Tung distribution function; dashed line, by the log-normal distribution function.

for PMI-18 by the Shulz summation method is well represented by this continuous function of Tung,[29] as can be easily seen by the agreement between the full line and the experimental results represented by the open circles in Figure 4.

Another useful function for describing the polymer molecular weight distribution is the log-normal distribution[30,31]

$$W(M) = (1/\beta)(1/M) \exp[-(1/\beta^2) \ln^2 (M/M_0)] \quad (5)$$

where β and M_0 are adjustable constants. This equation was derived from the normal distribution function by using the logarithm of the molecular weight as the independent variable. For polymers obeying this function a straight line is obtained by plotting the cumulative weight function $I(M)$ vs. the molecular weight on log-probability graph paper.[30] The constants β and M_0 can be obtained from the slope and the intercept of the straight line.

A plot of $I(M)$ from Schulz's summation method (Table I) represented according to this method is shown in Figure 5. The values determined from the best straight line are $\beta = 1.79395$ and $M_0 = 22.500$. Figure 6 shows the differential distribution curve (eq 5) calculated with these values of the parameters. The two methods give similarly shaped differential curves.

The number- and weight-average molecular weights of polymer PMI-18 can be calculated from these smoothed MWD functions. The expressions are as follows. For Tung's function

$$M_n = y^{-1/z}/[\Gamma(1 - 1/z)] \quad (6)$$

$$M_w = y^{-1/z}[\Gamma(1 + 1/z)] \quad (7)$$

and for the log-normal distribution

$$M_n = M_0 \exp(-\beta^2/4) \quad (8)$$

$$M_w = M_0 \exp(\beta^2/4) \quad (9)$$

Using the fitted values of z, y, β, and M_0, we obtain for M_n and M_w of the original polymer the results summarized in Table II.

However eq 6 cannot be applied to calculate M_n when z is equal to or less than 1. Furthermore, number-average molecular weights calculated from eq 6 are frequently much lower than the values calculated by direct summa-

Table II
Molecular Weight Averages M_w and M_n and M_w/M_n Ratio as Available Calculated for the PMI-18 Whole Sample on the Basis of Fractionation Data Obtained by Coacervation and GPC as Indicated in the Text

	method			
	A[a]	B[b]	C[c]	D[d]
$M_w \times 10^{-3}$	>43.6	44.4	50.5	57.4
$M_n \times 10^{-3}$	10.35		10.0	10.20
M_w/M_n			5.05	5.63

[a] Direct summation method from experimental M_n of fractions. [b] From Tung's treatment using coacervation data for fractions. [c] From log-normal distribution using coacervation data for fractions. [d] Direct summation method using for the fractions $(M_w)_{GPC}$ and $(M_n)_{GPC}$ calculated from GPC calibration.

tion from experimental distribution curves.[32,33] In the method of Tung,[29] M_n cannot be calculated because for our polymer, $z < 1$. M_n can be obtained directly from the experimental data of the fractions without recourse to any smoothed MWD function. According to its definition

$$M_n = [\sum_{i=1}^{N} w_i/(M_n)_i]^{-1} \quad (10)$$

where $(M_n)_i$ is the number-average molecular weight experimentally determined on fraction i and N is the total number of fractions ($N = 24$ in our case). The result thus obtained by direct weighted summation of the $(M_n)_i$'s of the fractions is shown in Table II. As we can see, the log-normal function estimates very accurately this "experimental" value of M_n. Since only values of $(M_n)_i$ have been determined experimentally, it is not possible to obtain M_w for the whole polymer by a similar direct summation of $(M_w)_i$'s of the fractions. We can approximate the true value of M_w only if we neglect the polydispersity of the fractions by the expression

$$M_w \simeq \sum_{i=1}^{N} w_i(M_n)_i \quad (11)$$

The result thus obtained is shown in Table II. The M_w estimated by the method of Tung[29] is very close to this one. Since $(M_w)_i > (M_n)_i$ for any i, the value of M_w obtained with eq 11 represents a lower bound for the true M_w, which should be higher.

We shall compare later all these results on M_n and M_w with the ones deduced from GPC data.

No corrections for dispersion or column broadening effects were made for the calculated GPC molecular weights determined in this work. It should be emphasized that the chromatograms for either the whole polymer or the fractions were not first corrected for Gaussian instrumental spreading as advocated by Tung et al.[34,35] Thus, the distributions reported here might be slightly broader than the true values. However, this correction is not important in polymers of broad molecular weight distributions,[34,35] and it only becomes increasingly important with increasingly narrow polymer fractions.

In addition, McCrackin[8,36] has demonstrated that for polydisperse fractions and columns similar to the ones employed in the present work no corrections for dispersion or column broadening effect for the calculated GPC molecular weights are needed.

The chromatogram corresponding to the whole polymer can be reconstructed from the chromatograms of the fractions and the result compared with the actual chromatogram determined on the unfractionate sample. For this comparison it is necessary to convert the individual GPC chromatograms to a base line linear in the same molecular weight average and to normalize the area under the curve. To perform this the gel permeation chromatograms of the fractions were sliced with vertical lines spaced at 1.5- and 2.0-mL elution volume intervals. The area of each slice was then calculated by direct measurement assuming the slice approximated a trapezoid. This method when it is checked by planimetry or direct weighing gives results of equal accuracy. The area defined by the trapezoid was taken as proportional to the weight fraction of the portion within the limits of molecular weight defining the slice. The weight fraction for the slice was then calculated. The whole chromatogram was rebuilt on the same molecular weight range of the whole polymer using the same scale.

Once we have the amount of material for each of the subfractions (slices) in units of weight fraction having volumes of elution between $V_e(n)$ and $V_e(n+1)$, the slices for all the fractions are summed to obtain normalized areas. Later these normalized areas are used to construct rectangles of equal area for each corresponding interval, keeping the base as in the original chromatograms and heights at the midpoint marked. A smooth curve was then drawn through each point in such a manner that the area of the rectangle outside the curve equals the area delimited by the curve, the line defining the interval terminus and half of the top side of the rectangle. The results of this procedure for PMI-18 are shown by the dashed line in Figure 1. It is obvious that in this case we do not need to make any refractive index increment difference corrections due to detector response as a function of molecular weight.

There are only small discrepancies between the trace of the original chromatogram and the one reconstructed from the chromatograms of the fractions. Probably they can be adequately exlained by considering only the yield of the fractionation.

The chromatograms of the different fractions of PMI-18 obtained by the coacervation method can be used to determine the molecular weight distribution of the polymer by GPC analysis. The elution volumes corresponding to the peaks of the fraction chromatograms, V_e(peak), are given in Table I and in Figure 3, where the log of the experimental M_n values of the fractions are plotted vs. V_e(peak). The conversion of elution volumes, V_e, into molecular weights, M, cannot be done directly from the log M_n vs. V_e(peak) correlation because the fractions are not monodisperse and they vary in polydispersity from sample to sample. Instead, an appropriate method of GPC calibration valid with polydisperse standards should be used.

Balke et al.[6] developed a computer method to obtain the calibration curve $\log M = f(V)$ with polydisperse standards in which two averages of molecular weight are required, but it was applied only to linear functions:

$$\log M = A_0 + A_1 V \quad (12)$$

As we see in Figure 3, our log M_n–V_e(peak) data cover a wide range of M over which deviations from linearity can be easily detected. McCrackin[8] described a method to include nonlinear effects by means of a quadratic curve

$$\log M = A_0 + A_1 V + A_2 V^2 \quad (13)$$

and Szewczyk[10,37] recently proposed an iterative method that can be applied to any polynomial of degree n:

$$\log M = A_0 + A_1 V + A_2 V^2 + \ldots + A_n V^n \quad (14)$$

This method of Szewczyk,[10,37] with degrees $n = 1$–3, is the one we have used here to determine the GPC calibration curve. The data required in this method are a known

average molecular weight M_i for each fraction i and the normalized chromatogram of the fraction, $H_i(V)$. In our case, $\bar{M} = M_n$.

It is supposed that the calibration curve, f, can be obtained from the known $\bar{M}$'s if a suitable averaged value of the elution volume, $\bar{V}$, is used for each sample. Therefore, for polydisperse calibrating samples, eq 14 reads

$$\log \bar{M} = f(\bar{V}) = A_0 + A_1\bar{V} + A_2\bar{V}^2 + ... + A_n\bar{V}^n \quad (15)$$

The average elution volumes are related to the molecular weight averages, M, by the inverse function, $\bar{V} = f^{-1}(\log \bar{M})$, which is written also as a polynomial of the same degree as f:

$$\bar{V} = f^{-1}(\log \bar{M}) = B_0 + B_1(\log \bar{M}) + B_2(\log \bar{M})^2 + ... + B_n(\log \bar{M})^n \quad (16)$$

Equations 15 and 16 are used to establish an iterative cycle that determines the A_k and B_k coefficients of f and f^{-1} (k = 1, 2, ..., n).

As starting values for $\bar{V}$, the peak elution volumes, V_e, are used in eq 15 and 16. By a least-squares fit of the log $\bar{M}$ vs. V_e data, the zeroth-order approximation to the coefficients A_k and B_k are determined. The goodness of the fit is gauged by means of the deviation:

$$\Delta = [(1/N)\sum_{i=1}^{N}(1 - \bar{M}_i^c/\bar{M}_i)^2]^{1/2} \quad (17)$$

Here, $\bar{M}_i^c$ is the value of $\bar{M}_i$ calculated from the chromatogram of fraction i and the fitted calibration curve f. For a number-average, $\bar{M}_i^c$ is obtained as

$$\bar{M}_i^c = (M_n)_i^c = \left\{\int_0^\infty [H_i(V)/M(V)]\, dV\right\}^{-1} \quad (18)$$

where $M(V)$ is given by $M(V) = 10^{f(V)}$ and $f(\bar{V})$ is given by eq 15 with the fitted A_k coefficients.

A new cycle in the iteration is started by calculating the average elution volumes, $\bar{V}$, from the $\bar{M}_i^c$'s:

$$\bar{V}_i = f^{-1}(\log \bar{M}_i^c) \quad (19)$$

with f^{-1} given by eq 16 and the B_k coefficients from the previous fit. The $\bar{V}$ values thus calculated are combined with the experimental $\bar{M}$'s to obtain a new set of A_k and B_k coefficients by a least-squares fit of log $\bar{M}$–$\bar{V}$, according to eq 15 and 16. The $\bar{M}_i^c$ and Δ are calculated anew and the cycle is reinitiated by obtaining $\bar{V}_i$'s from the $\bar{M}_i^c$'s. The iteration proceeds until a minimum in Δ is obtained.

The calculation of this iterative method has been programed in Fortran V using the routines of Sperry Univac's Large Scale Systems Math-Pack[38] for the least-squares fit to eq 15 and 16. In Figure 7 we show the root-mean-square deviation, Δ, obtained with polynomials of degree n = 1–3 plotted against the number of iterations. Iteration number zero means that the fit is done with the starting V_e values of Table I.

As we can see in Figure 7, the best fit is obtained with n = 2 after the first iteration (Δ = 0.118). The coefficients in eq 15 defining this best calibration curve are

$$A_0 = 5.09774$$
$$A_1 = 2.59575 \times 10^{-2} \quad (20)$$
$$A_2 = -2.21065 \times 10^{-4}$$

The curve is drawn as a full line in Figure 3. Also shown in the figure as a dashed line is the curve obtained with n = 1 after the first iteration.

Once the calibration curve has been established, it is possible to obtain the polydispersity of the fractions by

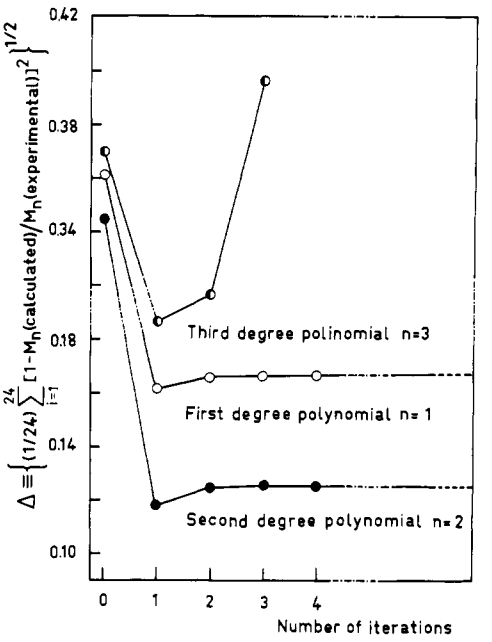

Figure 7. Root-mean-square deviation of the M_n values calculated with the calibrating equation relative to the experimental M_n's. The calibrating equation is a polynomial of the form $\log M = A_0 + A_1V_e + A_2V_e^2 + ... + A_nV_e^n$ and the fitting procedure is an iterative one described in the text. Iteration zero means that the experimental V_e(peak) and M_n(exptl) values are used as trial values directly.

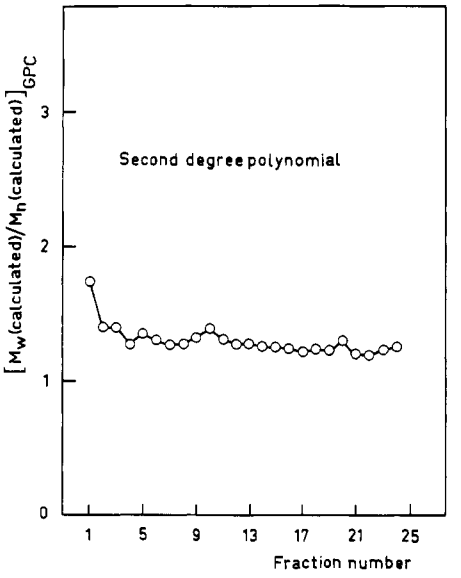

Figure 8. Polydispersity index of PMI-18 fractions. The circles represent values obtained with the second-degree polynomial after the first iteration as described in the text.

calculating their weight-average molecular weights, $(M_w)_i^c$, from the corresponding chromatograms by means of the following expression:

$$(M_w)_i^c = \int_0^\infty H_i(V)M(V)\, dV \quad (21)$$

with $M(V) = 10^{f(V)}$, as before, and $f(V)$ given by the best calibration function (coefficients (20) in eq 15). The values thus calculated for $(M_w)_i^c$ and the corresponding values of $(M_n)_i^c$, calculated according to eq 18 with the same f, are shown in Table I. The variation of $(M_w)_i^c/(M_n)_i^c$ from fraction to fraction is plotted in Figure 8. As we can see, the polydispersity index of the fractions is moderately low (1.2–1.4) and it varies in a progressive and smoothed way (the first fraction F-1 being an exception).

The polydispersity of the whole PMI-18 sample can also be obtained by a summation procedure from the GPC calibration curve. The number- and weight-average molecular weights of the whole original polymer (M_n and M_w) are related to the averages of the fractions $(M_n)_i^c$ and $(M_w)_i^c$ by means of the equations

$$M_n = [\sum_{i=1}^{N} w_i/(M_n)_i^c]^{-1} \quad (22)$$

$$M_w = \sum_{i=1}^{N} w_i(M_w)_i^c \quad (23)$$

The results thus obtained are shown in Table II, where they are compared with the ones obtained previously by direct summation of $(M_n)_i$'s and those estimated from the smoothed MWD functions fitted to coacervation data. The value calculated for M_n from GPC analysis agrees very well with the "experimental" one obtained by direct summation of the experimental $(M_n)_i$'s. The polydispersity index M_w/M_n from GPC is about 10% higher than that estimated by the log-normal function from coacervation. In general, the agreement between results obtained by different methods is satisfactory.

The universal calibration is based on the notion that the elution volume at the peak, V_e(peak), is a unique function of the hydrodynamic volume, V_h, of the eluting macromolecule.[11,12] V_h is given by the product of molecular weight and intrinsic viscosity, $[\eta]M$. Under fixed experimental conditions the relation between log $[\eta]M$ vs. V_e(peak) has been shown to be independent of polymer type and structure over a wide range.[12,39,40] However, there are a few reported well-established exceptions.[2,41,42] A branched macromolecule is more compact than its linear analogue and behaves in GPC like a linear macromolecule of smaller molar mass. With a few exceptions,[43,44] the universal calibration has been shown to be valid for branched molecules.[45] We test here whether such universal calibration is also valid for our comblike polymer PMI-18. To this end, we obtain the hydrodynamic volumes of the PMI-18 fractions and compare them with their corresponding GPC elution volumes at the peak, V_e(peak).

For polydisperse samples, there is no unique way for relating V_h to V_e(peak). It has been usually proposed that an average hydrodynamic volume, $\bar{V}_h$, should be used, calculated as

$$\bar{V}_h = [\eta]\bar{M} \quad (24)$$

where $\bar{M}$ is M_n, M_w, or $(M_nM_w)^{1/2}$. Schultz et al.[46] have proposed a GPC-average molecular weight, $\bar{M}_{GPC}$, calculated from the chromatogram by

$$\bar{M}_{GPC} = \int_0^\infty H(V)[M(V)]^{1+a}\,dV / \int_0^\infty H(V)[M(V)]^{a}\,dV \quad (25)$$

where K and a are the Mark–Houwink constants. Other authors[47] have preferred to use the hydrodynamic volume corresponding to the most probable molecular weight, namely

$$V_h^{mp} = KM_{mp}^{1+a} \quad (26)$$

where M_{mp} is the value of M at the maximum of the molecular weight distribution, which is made to correspond with the maximum in the chromatogram, or V_e(peak).[47]

In paper 2 of this series we report experimental results of $[\eta]$ for our PMI-18 fractions and obtain the corresponding K and a values. From such results we can now calculate the hydrodynamic volume by any one of the methods cited above. As we shall see in paper 2, K and a are not constant in our system. There are two sets of values for K and a, one (K_I and a_I) for $M < M_c$, and another (K_{II} and a_{II}) for $M > M_c$. From the double-logarithmic plot of $[\eta]$ vs. M_n, measured in THF, at 25 °C, for our fractions, we have determined (paper 2)[28] $M_c = 12\,500$, $K_I = 9.61 \times 10^{-3}$, $a_I = 0.674$, $K_{II} = 0.842$, and $a_{II} = 0.202$.

In view of the nonconstancy of K and a, the average in eq 25 has to be redefined. In a polydisperse sample, each of the monomolecular species has an elution volume, V, and a unique hydrodynamic volume, V_h, given by

$$V_h = [\eta](V)M(V) = K(V)[M(V)]^{1+a} \quad (27)$$

For the whole sample, we define the GPC average of V_h as the weighted sum of these individual V_h's, with the chromatogram taken as weighting function:

$$\bar{V}_h = \int_0^\infty H(V)K(V)[M(V)]^{1+a}\,dV \quad (28)$$

Likewise, the measured $[\eta]$ is given by the average

$$[\bar{\eta}] = \int_0^\infty H(V)K(V)[M(V)]^{a}\,dV \quad (29)$$

so that in the case of K and a nonconstant, $\bar{M}_{GPC}$ is to be calculated according to

$$\bar{M}_{GPC} = \bar{V}_h/[\bar{\eta}] \quad (30)$$

(with $\bar{V}_h$ and $[\bar{\eta}]$ given by eq 28 and 29) instead of according to eq 25.

We have calculated $\bar{V}_h$ and $\bar{M}_{GPC}$ using eq 28–30, with the K and a values given in paper 2. $H(V)$ is taken from the normalized chromatograms and the function $M(V)$ is obtained from the best calibration curve determined above. The results of $\bar{M}_{GPC}$ are shown in Table I (column 9) and the results of $\bar{V}_h$ are shown in Figure 9 compared with those relative to PS standards.

The universal calibration plot was also constructed with PS standards. Thus the product $V_h = [\eta]M$(peak) was also plotted in Figure 9. M_w and M_n given by the suppliers were used for M(peak) $= (M_wM_n)^{1/2}$ and $[\eta]$ was then calculated from this M(peak) through the Mark–Houwink equation[48] in THF at 25 °C, $[\eta] = 1.60 \times 10^{-2}M^{0.706}$. For almost monodisperse samples these two approximations do not introduce significant differences in the final value plotted for the hydrodynamic volume, V_h.

The V_e(peak) dependencies of $V_h = [\eta]M$(peak) for polystyrene and of $\bar{V}_h = [\bar{\eta}]\bar{M}_{GPC}$ for PMI-18 fractions are slightly different, the deviations being higher in the region of high molecular weights. This behavior is understandable because PMI-18 undergoes structural changes from the low to the high molecular weight region.[28,49] However, sample polydispersity may also have some influence on this trend, since the polydispersity index of our fractions is not constant but increases slightly with molecular weight (Figure 8).

Often, the average molecular weight that is used together with $[\eta]$ to obtain $\bar{V}_h$ for universal calibration is M_n, M_w, or a combination of both, $(M_wM_n)^{1/2}$, as we just have mentioned above for the PS standards. It can be easily shown that $M_w < M_{GPC} < M_z$ for $0 < a < 1$. Therefore, use of M_n, M_w, or $(M_wM_n)^{1/2}$ instead of $\bar{M}_{GPC}$ would produce $\bar{V}_h$ values lower than the ones of Figure 9 and, hence, still larger deviations from the PS calibration curve.

If the molecular weight distribution is known, it is possible to use the hydrodynamic volume that corresponds to the most probable molecular weight,[47] i.e., eq 26. For our PMI-18 fractions we calculate M_{mp} by putting $V = V_e$(peak) in the $M(V)$ function determined by the calibration procedure described above. With these M_{mp}'s and the K and a values from paper 2, we obtain V_h^{mp} through

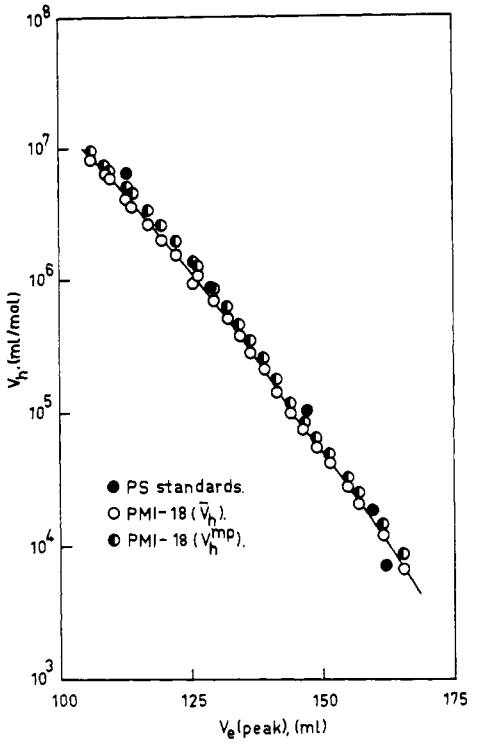

Figure 9. Universal calibration as a semilogarithmic plot of the hydrodynamic volume V_h vs. elution volume at the peak, V_e(peak), for polystyrene standards and a series of PMI-18 fractions in THF at 25 °C: full circles, polystyrene standards with $V_h = [\eta](M_w M_n)^{1/2}$; open circles, poly[*N*-(*n*-octadecyl)maleimide] fractions with $V_h = \bar{V}_h = [\bar{\eta}]\bar{M}_{GPC}$; half-filled circles, poly[*N*-(*n*-octadecyl)maleimide] fractions with $V_h = V_h^{mp} = KM_{mp}^{1+a}$. The full line has been drawn through the $\bar{V}_h$ points.

eq 26. The results of V_h^{mp} are slightly larger than the ones of $\bar{V}_h$ shown in Figure 9. Typically, log V_h^{mp} values are about 0.04–0.10 larger than those of log $\bar{V}_h$. When plotted against V_e(peak), they still do not lie over the PS calibration curve.

These deviations are in agreement with observations made by some authors[44,50] that some stiff-chain macromolecules deviate from the universal calibration plot. However, which of the factors outlined in the Introduction of this paper operates has yet to be explained. At present we have insufficient data to elucidate which of them may be operative since anomalous effects in GPC of systems departing from universal calibration do not always operate in the same direction.

Acknowledgment. Thanks are due to Dr. M. Criado-Sancho (UNED) for help with the computing work. C.R.G. gratefully acknowledges support of this work by a grant from the Consejo Superior de Investigaciones Cientificas. J.M.B.-R. is grateful also to the Comision Asesora de Investigación Científica del Ministerio de Universidades e Investigación for partial support (Grants-in-Aid for Scientific Research 3363/79 and 0077/81) of this research.

Registry No. Poly[*N*-(*n*-octadecyl)maleimide], 26714-93-2.

References and Notes

(1) Dawkins, J. V., quoted by Bevington, J. C.; Dyball, C. J. *J. Polym. Sci., Polym. Chem. Ed.* **1976**, *14*, 1819.
(2) Mencer, H. J.; Grübisic-Gallot, Z. *J. Liq. Chromatogr.* **1979**, *2*, 649.
(3) Moore, J. C. *J. Polym. Sci., Part A* **1964**, *2*, 825.
(4) Cantow, M. J. R.; Porter, R. S.; Johnson, J. F. *J. Polym. Sci., Part A-1* **1967**, *5*, 1391.
(5) Frank, F. C.; Ward, I. M.; Williams, T. J. *J. Polym. Sci., Part A-2* **1968**, *6*, 1357.
(6) Balke, S. T.; Hamielec, A. E.; LeClair, B. P.; Pearce, S. L. *Ind. Eng. Chem. Prod. Res. Dev.* **1969**, *8*, 54.
(7) Weiss, A. R.; Cohn-Ginsberg, E. *J. Polym. Sci., Part A-2* **1970**, *8*, 148.
(8) McCrackin, F. L. *J. Appl. Polym. Sci.* **1977**, *21*, 191.
(9) Yau, W. W.; Stoklosa, H. J.; Bly, D. D. *J. Appl. Polym. Sci.* **1977**, *21*, 1911.
(10) Szewczyk, P. *Polymer* **1976**, *17*, 90.
(11) Benoit, H.; Grübisic-Gallot, Z.; Rempp, P.; Decker, D.; Zilliox, J. G. *J. Chim. Phys. Phys.-Chim. Biol.* **1966**, *63*, 1507.
(12) Grübisic-Gallot, Z.; Rempp, P.; Benoit, H. *J. Polym. Sci., Part B* **1967**, *5*, 753.
(13) Heufer, G.; Braun, D. *J. Polym. Sci., Part B* **1965**, *3*, 495.
(14) Segal, L. *J. Polym. Sci., Part B* **1966**, *4*, 1011.
(15) Harmon, D. J. *J. Polym. Sci., Part C* **1965**, *8*, 243.
(16) Nakajima, N. *J. Polym. Sci., Part A-2* **1966**, *5*, 101.
(17) Meyerhoff, G.; Jovanovic, S. *J. Polym. Sci., Part B* **1967**, *5*, 495.
(18) Rohn, C. L. *J. Polym. Sci., Part A-2* **1967**, *5*, 547.
(19) MacCallum, D. *Makromol. Chem.* **1967**, *100*, 117.
(20) Alliet, D. F.; Pacco, J. M. *J. Polym. Sci., Part C* **1968**, *21*, 199.
(21) Dawkins, J. V. *Polymer* **1978**, *19*, 705.
(22) Dawkins, J. V. *Pure Appl. Chem.* **1979**, *51*, 1473.
(23) Audebert, R. *Polymer* **1979**, *20*, 1561.
(24) Gonzalez Ramos, J.; Barrales-Rienda, J. M.; Sánchez Chaves, M. *An. Quim.* **1977**, *73*, 139.
(25) Barrall, E. M., II; Cantow, M. J. R.; Johnson, J. F. *J. Appl. Polym. Sci.* **1968**, *12*, 1373.
(26) Schulz, G. V.; Dinglinger, A. *Z. Phys. Chem.* **1939**, *B43*, 47.
(27) Schulz, G. V. *Z. Phys. Chem.* **1940**, *B47*, 155.
(28) Barrales-Rienda, J. M.; Romero Galicia, C.; Freire, J. J.; Horta, A. *Macromolecules*, companion paper in this issue (Part 2).
(29) Tung, L. H. *J. Polym. Sci.* **1956**, *20*, 495.
(30) Lansing, W. D.; Kraemer, E. O. *J. Am. Chem. Soc.* **1935**, *57*, 1369.
(31) Wesslau, H. *Makromol. Chem.* **1956**, *20*, 111.
(32) Howard, G. J. *J. Polym. Sci.* **1962**, *59*, S1.
(33) Green, J. H. S.; Paisly, H. M. *Research* **1961**, *14*, 170.
(34) Tung, L. H.; Runyon, J. R. *J. Appl. Polym. Sci.* **1969**, *13*, 775.
(35) Tung, L. H.; Runyon, J. R. *J. Appl. Polym. Sci.* **1969**, *13*, 2397.
(36) Fetters, L. J. *J. Appl. Polym. Sci.* **1976**, *20*, 3437.
(37) Szewczyk, P. *J. Polym. Sci., Part C* **1980**, *68*, 191.
(38) Routines ORTHLS, COEFS, FITD, and FITY.
(39) Boni, K. A.; Sliemers, F. A.; Stickney, P. B. *J. Polym. Sci., Part A-2* **1968**, *6*, 1759.
(40) Coll, H.; Gilding, D. K. *J. Polym. Sci., Part A-2* **1970**, *8*, 89.
(41) Dawkins, J. V.; Hemming, M. *Makromol. Chem.* **1975**, *176*, 1777.
(42) Dubin, P. L.; Koontz, S.; Wright, K. L., III *J. Polym. Sci., Polym. Chem. Ed.* **1977**, *15*, 2047.
(43) Pannell, J. *Polymer* **1972**, *13*, 277.
(44) Ambler, M. R.; McIntyre, D. *J. Polym. Sci., Part B* **1975**, *13*, 589.
(45) Wild, L.; Guliana, R. *J. Polym. Sci., Part A-2* **1967**, *5*, 1087.
(46) Shultz, A. R.; Bridgman, A. L.; Hadsell, E. M.; McCullough, C. R. *J. Polym. Sci., Part A-2* **1972**, *10*, 273.
(47) Lecacheux, D.; Lesec, J.; Quivoron, C. *J. Liq. Chromatogr.* **1982**, *5*, 217.
(48) Provder, T.; Rosen. E. M. *Sep. Sci.* **1970**, *5*, 437.
(49) Freire, J. J.; Barrales-Rienda, J. M.; Romero Galicia, C.; Horta, A. *Macromolecules*, companion paper in this issue (Part 3).
(50) Meyerhoff, G. *Makromol. Chem.* **1970**, *134*, 129.